Science Advances
AAAS

Supplementary Materials for

Regulation of developmental hierarchy in *Drosophila* neural stem cell tumors by COMPASS and Polycomb complexes

Cassandra Gaultier, Sophie Foppolo, Cédric Maurange*

*Corresponding author. Email: cedric.maurange@univ-amu.fr

Published 11 May 2022, *Sci. Adv.* **8**, eabi4529 (2022)
DOI: 10.1126/sciadv.abi4529

The PDF file includes:

Figs. S1 to S10
Legends for data S1 to S4

Other Supplementary Material for this manuscript includes the following:

Data S1 to S4

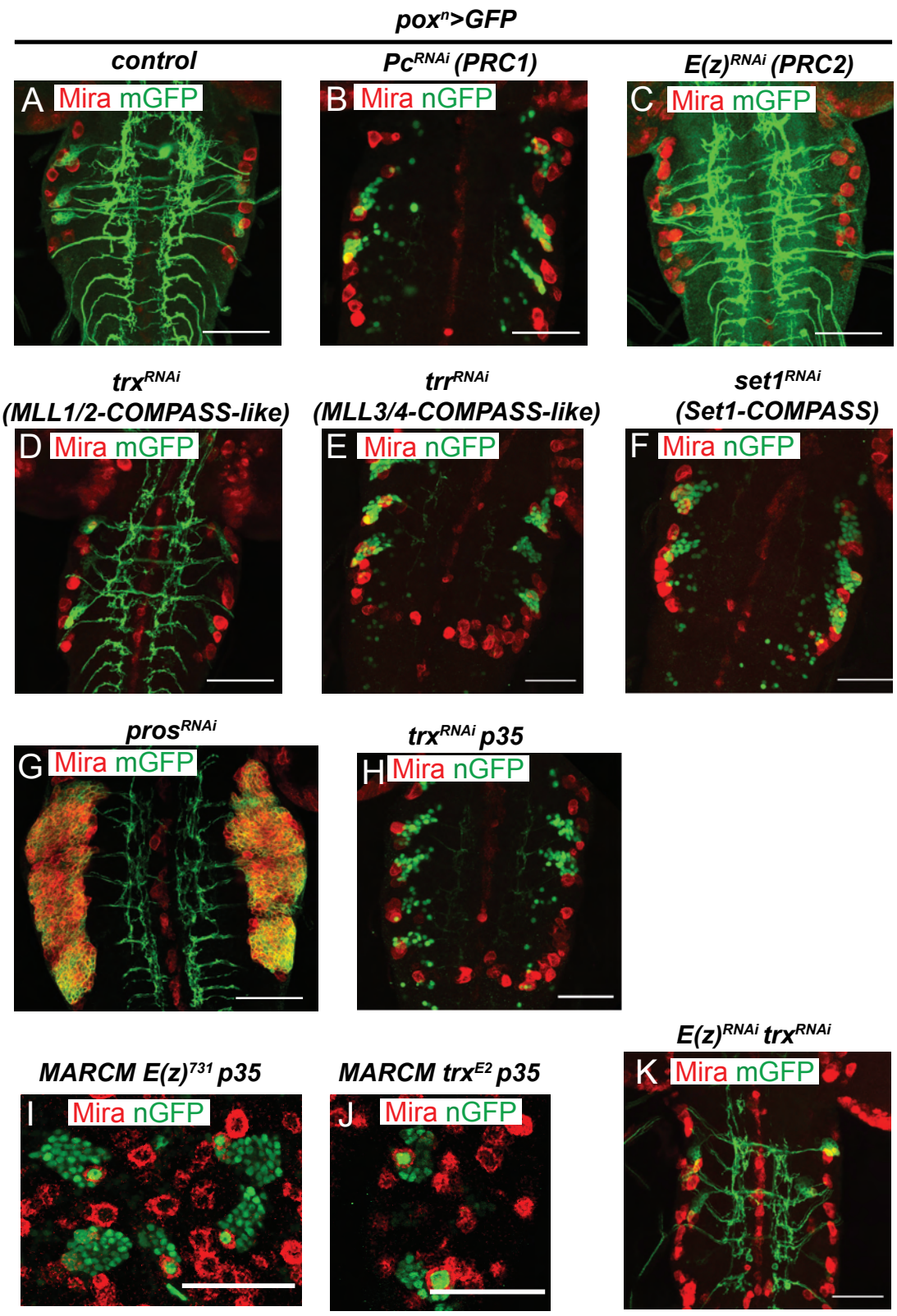
pox^n>GFP
control
A Mira mGFP
Pc^RNAi (PRC1)
B Mira nGFP
E(z)^RNAi (PRC2)
C Mira mGFP
trx^RNAi
(MLL1/2-COMPASS-like)
D Mira mGFP
trr^RNAi
(MLL3/4-COMPASS-like)
E Mira nGFP
set1^RNAi
(Set1-COMPASS)
F Mira nGFP
pros^RNAi
G Mira mGFP
trx^RNAi p35
H Mira nGFP
E(z)^RNAi trx^RNAi
K Mira mGFP
MARCM E(z)^731 p35
I Mira nGFP
MARCM trx^E2 p35
J Mira nGFP

Fig. S1. Knockdown of PRC1, PRC2 and COMPASS-like genes in larval NBs does not induce NB amplification and tumorigenesis

(**A**) Anti-Mira and anti-GFP immunostaining in late L3 *pox^{n}-GAL4; UAS-GFP* larvae. Membrane-bound GFP (mGFP) labels six lineages (NBs and their immediate GMCs and neuronal progeny) in the VNC.

(**B-F**) Anti-Mira and anti-GFP immunostaining in late L3 *pox^{n}-GAL4; UAS-GFP* larvae that also carry an RNAi transgene against representative members of *PRC1*, *PRC2* and *COMPASS* genes (*Polycomb* (*Pc*), *Enhancer of zeste* (*E(z)*), *trithorax* (*trx*), *trithorax-related* (*trr*) and *SET domain containing 1* (*set1*)). No NB amplification and tumorigenesis is observed. Nuclear GFP (nGFP) labels six lineages (NBs and their immediate progeny) in the VNC.

(**G**) Anti-Mira and anti-GFP immunostaining in late L3 *pox^{n}-GAL4; UAS-GFP* larvae that also carry an RNAi transgene against *prospero* (*pros*). *pros* inactivation in early larvae triggers NB amplification and tumorigenesis.

(**H**) RNAi-mediated co-inactivation of *E(z)* and *trx* does not trigger NB amplification.

(**I**) RNAi-mediated inactivation of *trx* and inhibition of apoptosis by mis-expression of p35 does not cause NB amplification.

(**J-K**) MARCM clones are labelled with nGFP. Clones mis-express p35 and are null mutant for either *E(z)* or *trx*. Inhibition of apoptosis in the context of *E(z)* and *trx* inactivation does not cause NB amplification.

Images are projection of several confocal sections, except I and J that are single confocal sections. Scale bars: 50 μm.

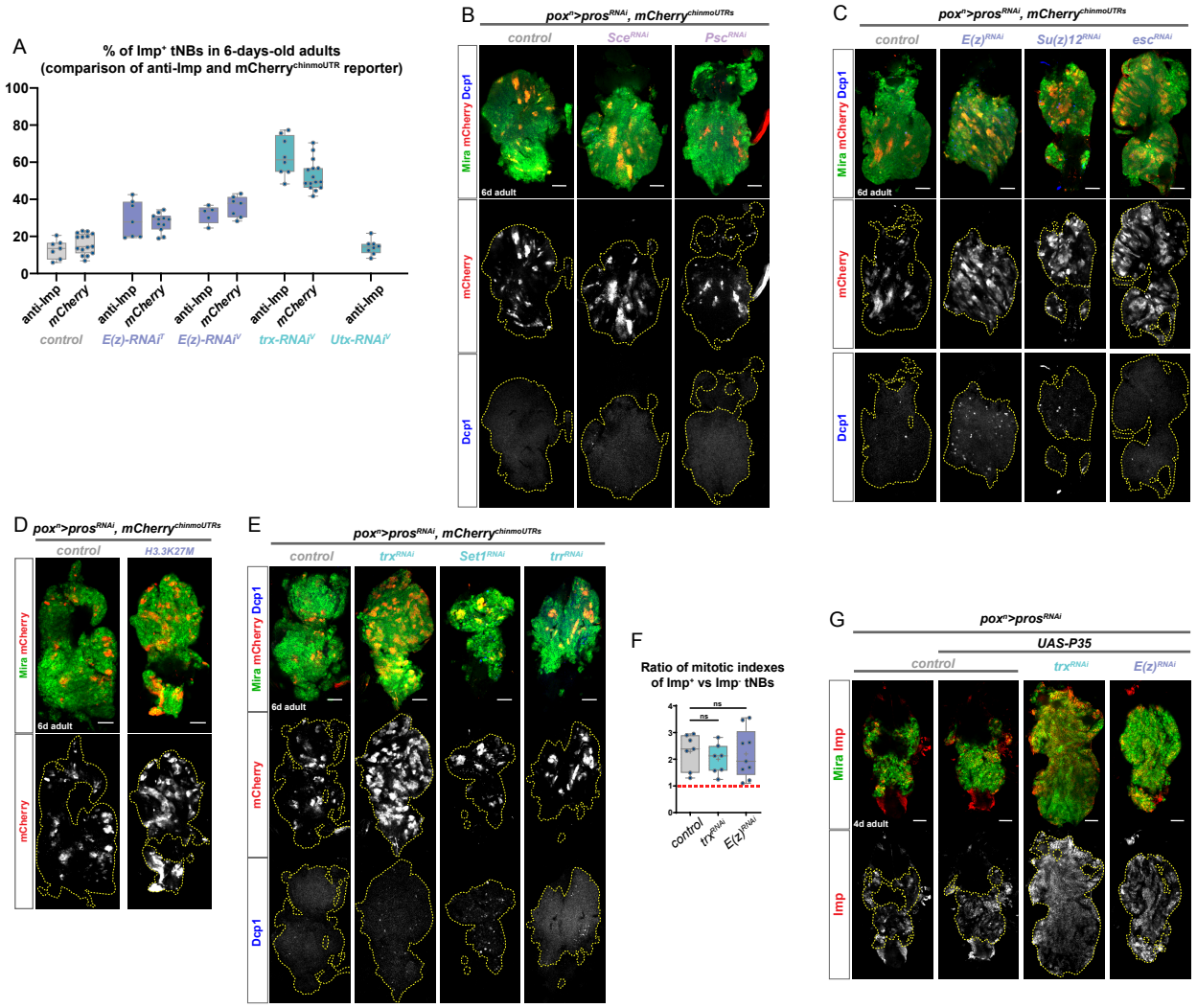

Fig. S2. Assessing the proportion of Imp$^+$ tNBs and the size of *pros^{RNAi}* tumors after inactivation of *COMPASS* and *Polycomb-Group* genes

(**A**) Box plots recapitulating quantifications of proportions of Imp$^+$ tNBs for *pox^n>pros^{RNAi} control* tumors compared to *pox^n>pros^{RNAi}* tumors with the additional RNAi-mediated knockdown of various members of the PRC2 and COMPASS groups. All measurements are made in tumors that persist in 6-day-old adults. Imp$^+$ tNBs are identified using anti-Imp or anti-mCherry immunostainings. mCherry reflects expression of Chinmo (*21*, *58*).

(**B-E**) *Control pox^n>pros^{RNAi}* tumors or *pox^n>pros^{RNAi}* tumors with RNAi-mediated inactivation of PRC1 genes (*Sce, Psc)* in (B), PRC2 genes (*E(z)*, *Su(z)12*, *esc*) in (C), or H3K4 methyl-transferases (*trx*, *Set1*, *trr*) in (E). In (D), control tumors are compared with tumors mis-expressing a mutated form of H3.3K27M. For (B), (C), (D) and (E), immunostainings against Mira (green) label all tNBs. Imp$^+$ tNBs are identified via an immunostaining against mCherry that labels the mCherry from the *UAS-mCherry^{chinmoUTRs}* transgene reflecting Chinmo expression.

(**F**) The ratio for each condition depicts the number of mitotic cells (PH3$^+$) per unit of volume of Imp$^+$ tNBs over the number of mitotic cells per unit of volume of Imp$^-$ tNBs. tNBs are labelled with Mira and Imp. One unit of volume = 10000 µm^3.

(**G**) Mis-expression of p35 in *control* $pox^{n}>pros^{RNAi}$ or $pox^{n}>pros^{RNAi,}$ trx^{RNAi} or $pox^{n}>pros^{RNAi,}$ $E(z)^{RNAi}$. Imp^{+} tNBs are identified via an immunostaining against Imp.
Scale bars, 50 µm. The dashed lines delimit the area of the tumor in the VNC of 6-day-old adults. Images are single confocal sections.

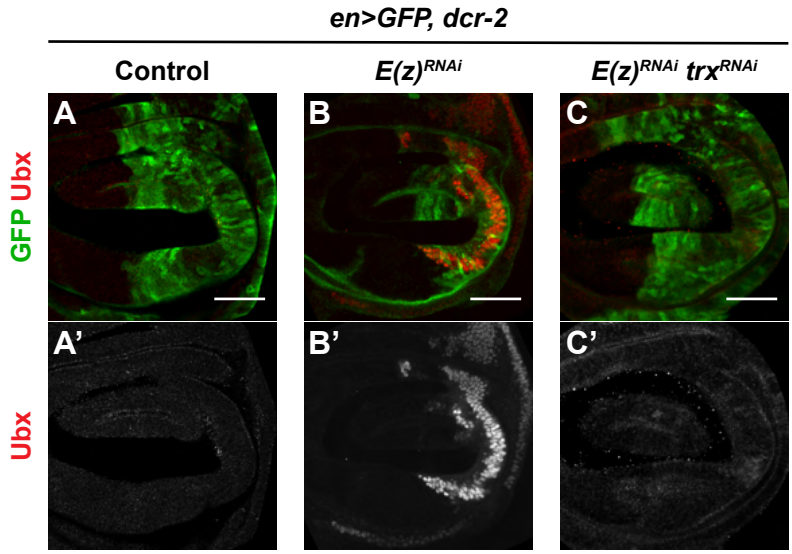

Fig. S3. Antagonistic phenotypes upon RNAi-mediated inactivation of *E(z)* and *trx* in larval imaginal discs
(**A**) Late L3 wing imaginal disc labelled with anti-GFP labelling the posterior compartment (*UAS-dcr-2, en-GAL4; UAS-GFP*).
(**B**) Upon *E(z)* knockdown via RNAi in the posterior compartment, Ubx is derepressed (*UAS-dcr-2, en-GAL4; UAS-GFP, UAS-*$E(z)^{RNAi}$).
(**C**) Upon co-inactivation of *E(z)* and *trx* via RNAi in the posterior compartment, silencing of Ubx is restored (*UAS-dcr-2, en-GAL4; UAS-GFP, UAS-*$E(z)^{RNAi}$*, UAS-*trx^{RNAi}). Ubx is marked using an anti-Ubx antibody.
Images are single confocal sections. Scale bars: 50 µm.

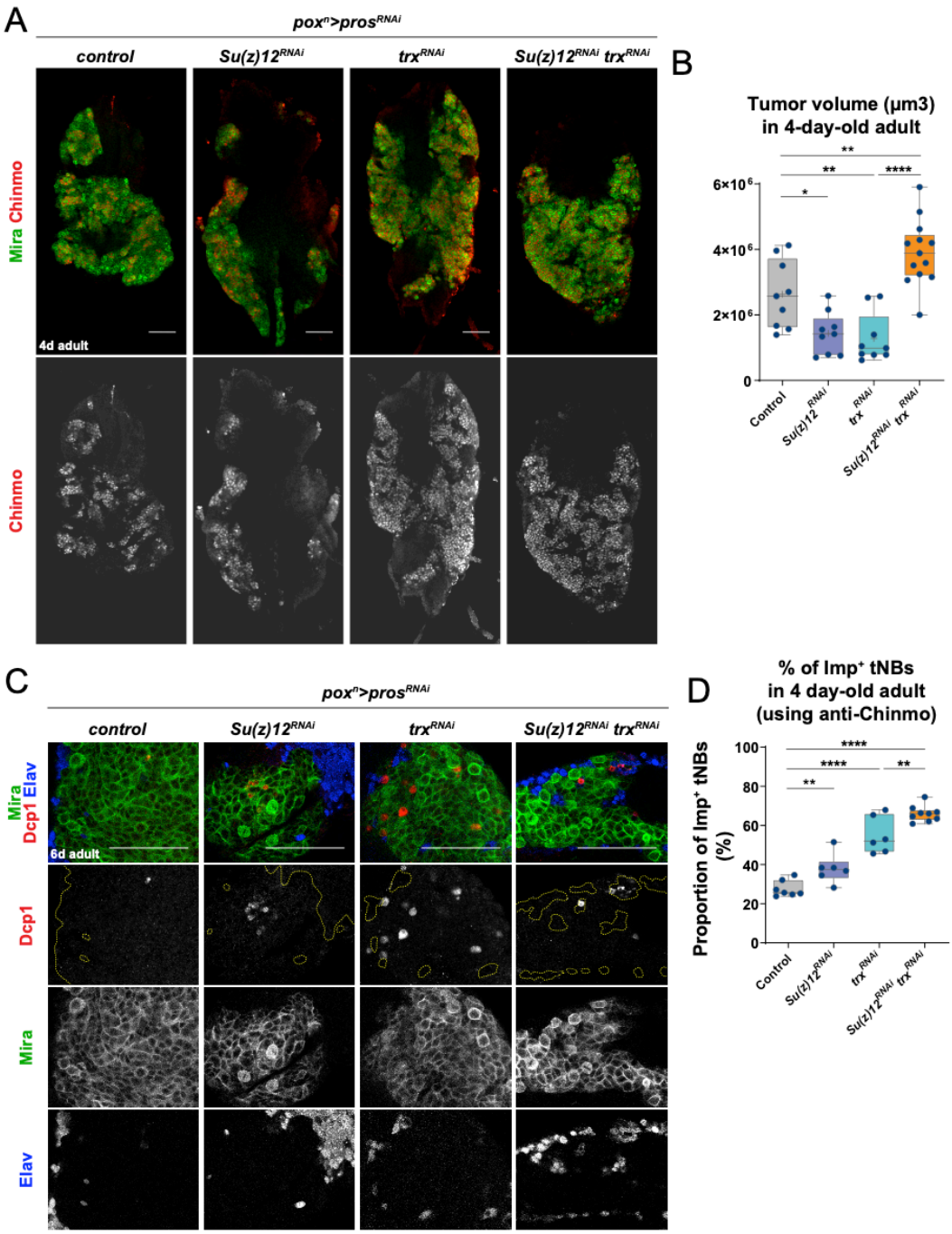

Fig. S4. Co-inactivation of *Su(z)12* and *trx* acts synergistically to increase the proportion of Imp$^+$ tNBs and amplify tumor growth

(**A**) *Control pox^n>pros^{RNAi}* tumors or *pox^n>pros^{RNAi}* tumors with RNAi-mediated inactivation of *Su(z)12* or *trx*, or co-inactivation of *trx* and *Su(z)12*. Immunostainings against Mira (green) labels all tNBs. Immunostainings against Chinmo (red) label the sub-population of Imp$^+$ tNBs. Images are single confocal sections of tumors in the VNC of 4-day-old adults. Scale bars: 50µm.

(**B**) Box plots recapitulating quantifications of tumor volumes (µm^3) for the genotypes indicated in (A). Tumor volume measurements are made based on anti-Mira immunostaining.

(**C**) Immunostainings of tumors showing apoptotic cells with anti-Dcp1 antibody. Apoptosis is strongly reduced upon co-inactivation of *Su(z)12* and *trx* compared to the single inactivation of *Su(z)12* or *trx*. The dashed lines delimit the area of the tumor in the VNC of 1-day-old adults. Scale bars: 50µm

(**D**) Box plots recapitulating quantifications of proportions of Imp^+ tNBs for the genotypes indicated in (A). Imp^+ tNBs are identified with an anti-Chinmo antibody.

Images are single confocal sections

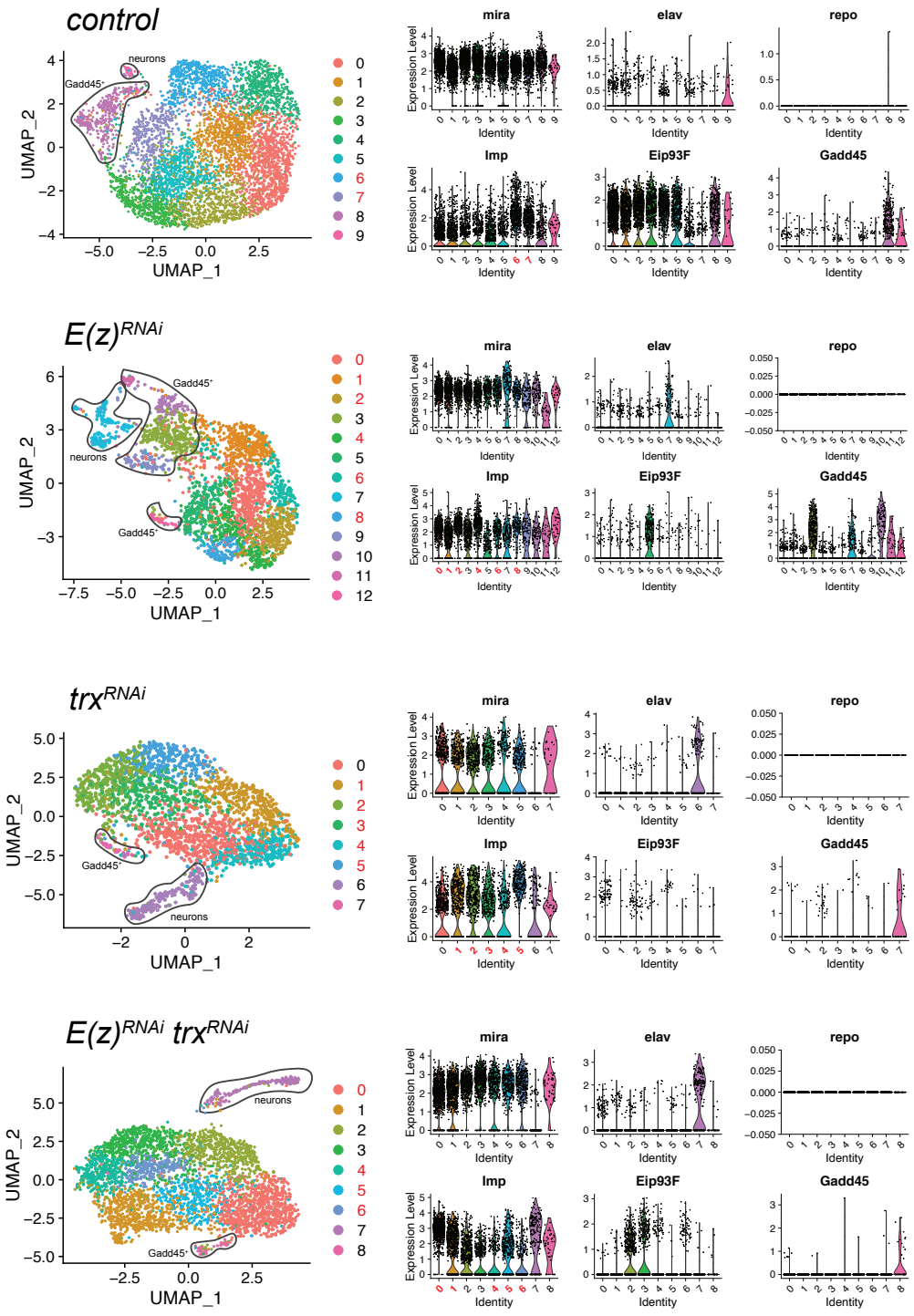

Fig. S5. Single-cell RNA-seq of four types of NB tumors

For each condition, sequenced cells were partitioned into 8 to 13 clusters using Seurat and visualized on UMAP plots. Violin plots indicate RNA levels of the selected gene for each cluster. Outlying clusters with high levels of Gadd45 or elav are delineated by a dotted line.

Clusters whose identity is highlighted in red exhibit high levels of Imp and low levels of Gadd45 or elav. These clusters were selected for further bioinformatic analyses as seen in Figure 6.

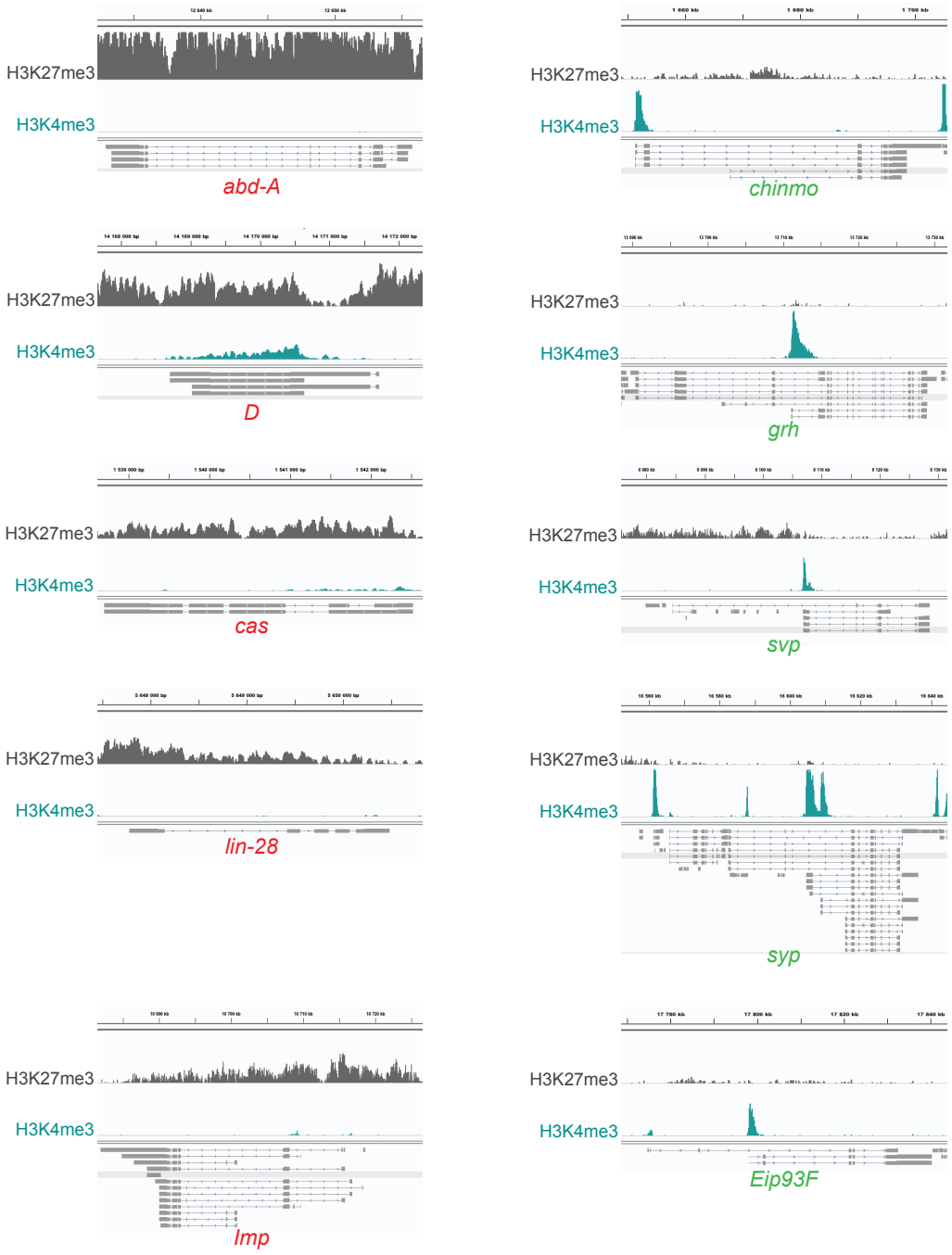

Fig. S6. Active and repressive histone modifications on temporal patterning genes in late larval NBs

Plots represent ChIP-seq tracks for the repressive and active histone marks (H3K27me^3 and H3K4me^3 respectively) for *abd-A*, a canonical target of TrxG and PcG complexes, and temporal patterning genes. ChIP-seq were performed in late L3 NBs. Genes exhibiting a strong repressive mark are labelled in red. Genes exhibiting a strong active mark are labelled in green. Except for chinmo that is post-transcriptionally regulated in larval NBs, the type of histone mark correlates with the gene expression state in NBs. Data were extracted from (*50*).

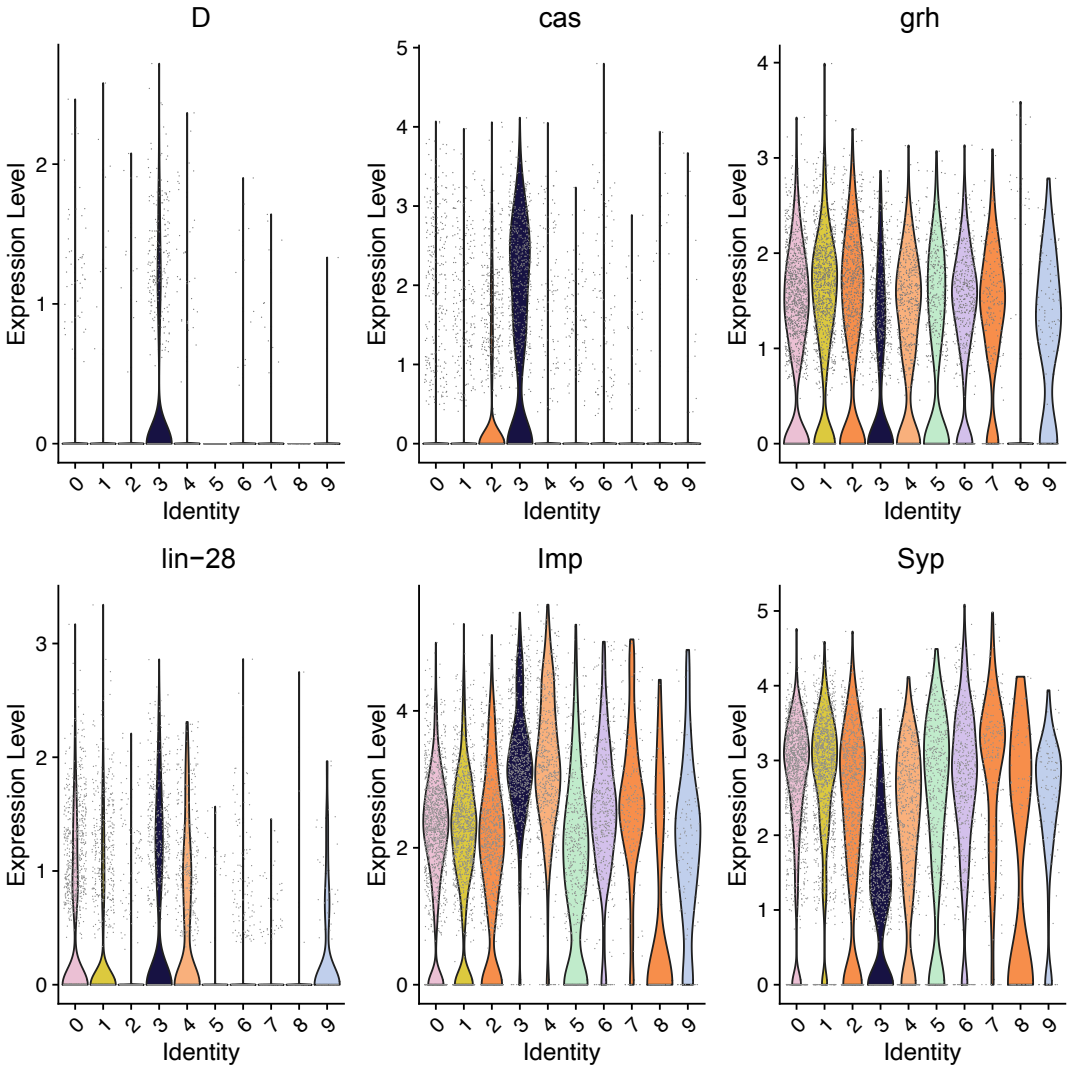

Fig. S7. Differentially expressed genes in the various UMAP clusters defining the merged population of Imp$^+$ tNBs

Violin plots depicting the expression levels of temporal patterning genes for each cluster.

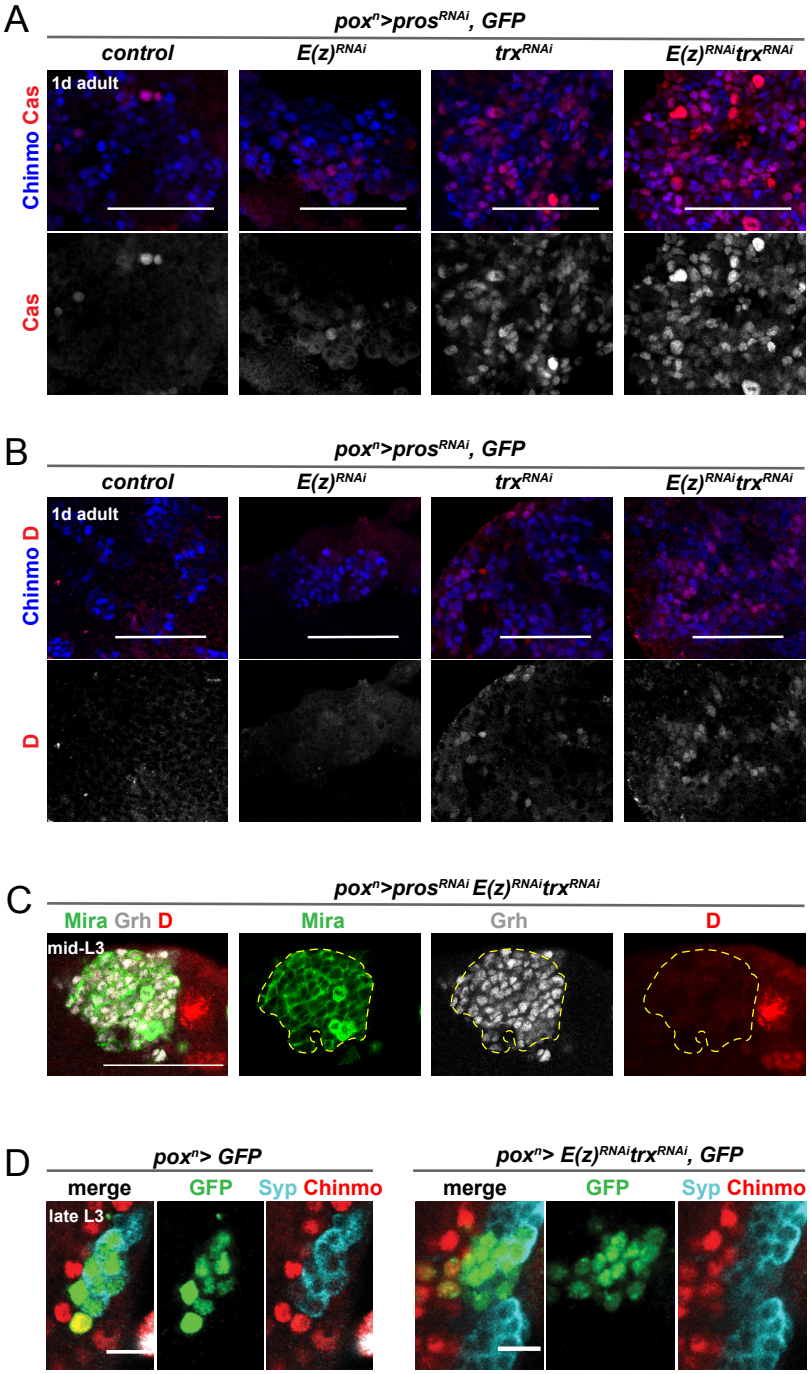

Fig. S8. Embryonic temporal identity markers are derepressed in *trx*^{RNAi} and *E(z)*^{RNAi}*trx*^{RNAi} tumors in adults but not in larvae

(**A**-**B**) Immunostainings against Cas and D indicate that the two genes are consistently derepressed in *trx*^{RNAi} and *E(z)*^{RNAi}*trx*^{RNAi} tumors. Chinmo labels Imp^{+} tNBs.

(**C**) *E(z)*^{RNAi}*trx*^{RNAi} NB tumor in mid-L3. The tumor is delineated by the dotted yellow line. tNBs are labelled with anti-Mira. Immunostainings against Grh and D indicate that all tNBs express Grh and none express D at this stage.

(**D**) GFP labels neurons produced by the *pox*^{n} NB during larval stages. The pox^{n} NB produces Chinmo^{+} early-born neurons and Syp^{+} late-born neurons. Upon knockdown of *trx* and *E(z)*, the pox^{n} NB remains able to generate both early and late neuronal subtypes. Scale bars are 50 µm for (A-C) and 10 µm for (D)

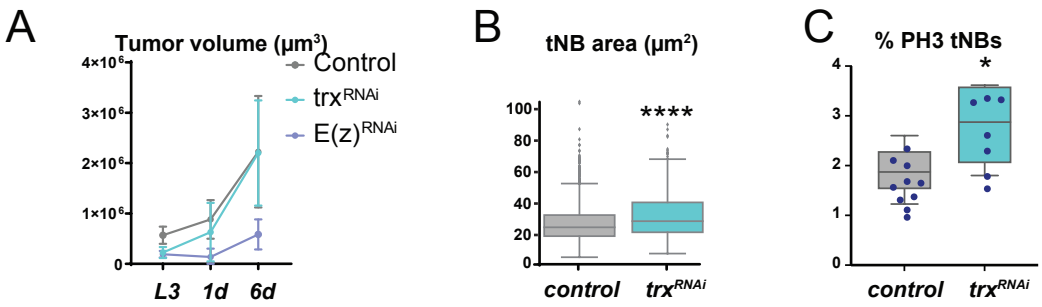

Fig. S9. Dynamics of tumor growth

(**A**) Evolution of tumor volume for the *control*, in *E(z)*^{RNAi} and *trx*^{RNAi} conditions from late L3 to 6-day-old adults.

(**B**) The area of tNBs in *trx*^{RNAi} tumors in 6-days old adults is on average about 20% larger than tNBs in the *control* condition (32,26 µm^2 (n = 801) vs 27,05 µm^2 (n=3014)). This is consistent with the fact that *trx*^{RNAi} tumors are enriched in Imp^{+} tNBs and with our previous finding that Imp^{+} tNBs are larger than Syp+ tNBs (*21*).

(**C**) Percentage of PH3^{+} tNBs in tumors. To obtain an approximation of the number of tNBs per tumor, the tumor volume was divided by the tNB average volume extrapolated from the average surface measured in (E).

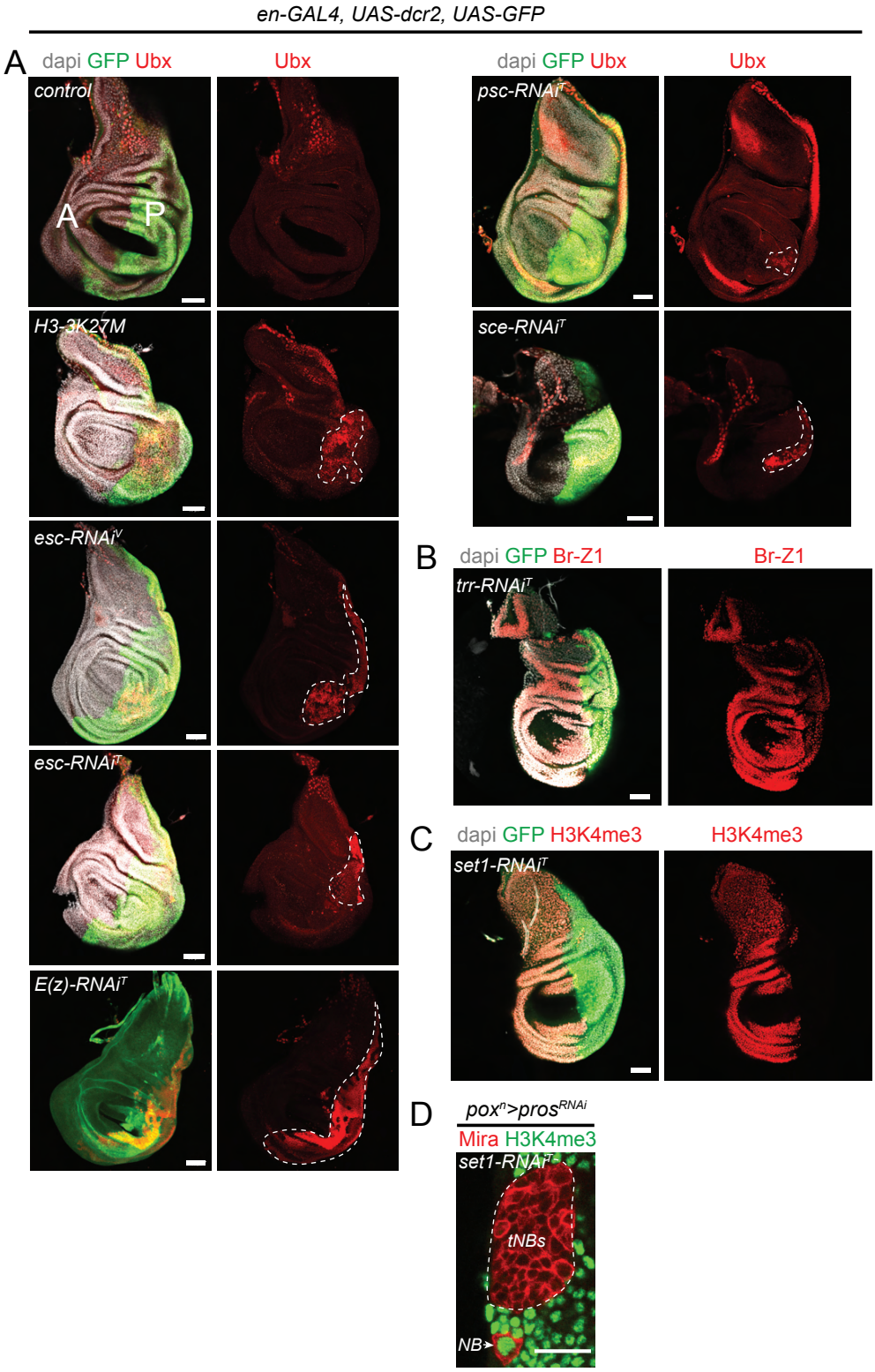

Fig. S10. Validation of RNAi lines

RNAi transgene expression was induced in the posterior compartment of the wing disc using engrailed-GAL4 (en-GAL4). A is for anterior, P is for posterior. GFP labels the posterior compartment.

(A) Knockdown of PRC2 genes is known to trigger derepression of the Hox gene *Ultrabithorax* (*Ubx*) in the wing disc (*80*). We tested RNAi lines for PRC2 genes. RNAi transgenes expression was induced using engrailed-GAL4 (en-GAL4).
(B) *trr* knockdown prevents expression of the ecdysone receptor target Br-Z1 (*81*).
T in uppercase indicates RNAi lines from the Transgenic RNAi Project (TRiP) provided by the Bloomington Stock Center, while V in uppercase indicates RNAi lines from the Vienna Drosophila Resource Center (VDRC).
(C) *set1* knockdown abrogates H3K4me3 deposition in the posterior compartment of the wing disc. (*54*)
(D) *set1* knockdown in late larval $pox^{n}>pros^{RNAi}$ tumors abrogates H3K4me3 deposition in tNBs (delineated by the dotted line). In contrast, H3K4me3 staining is strong in pox^{n}-negative NBs that don't express $set1^{RNAi}$ (arrow).

Data S1. (separate file)
Differentially expressed genes in $E(z)^{RNAi}$, trx^{RNAi} or $E(z)^{RNAi}trx^{RNAi}$ adult tumors compared to control adult tumors.
Temporal patterning genes are highlighted in red.

Data S2. (separate file)
Differentially expressed genes in Imp^{+} tNBs of the $E(z)^{RNAi}$, trx^{RNAi} or $E(z)^{RNAi}trx^{RNAi}$ adult tumors compared to *control* adult tumors.
Temporal patterning genes are highlighted in red.

Data S3. (separate file)
Enriched genes in each cluster composing the merge population of Imp^{+} tNBs

Data S4. (separate file) Codes for Seurat and Monocle